Study on the Operation of a Low-Voltage AC Microgrid with Multiple Distributed Generations

WEI-TZER HUANG
Department of Electrical Engineering
Chienkuo Technology University
No. 1, Chieh Shou N. Rd., Changhua City TAIWAN
vichuang@ctu.edu.tw

Abstract: - This paper aims to study the operation of a grid-connected low-voltage AC microgrid with multiple distributed generations (DGs). First of all, a 400 V low-voltage AC microgrid integrated with a 30 kW microturbine generator, a 13 kW photovoltaic generation system, a 10 kW fuel cell generation system, and a 10 kVA wind turbine generator was employed as the sample system. Next, a sequential three-phase power-flow program that developed by the implicit Z_{BUS} Gauss method was derived in this paper. Finally, the daily transformer loadings, voltage profiles, line flow profiles, and system losses of the proposed microgrid were analyzed and discussed by the developed sequential three-phase power-flow program. The outcomes of this paper are helpful for engineers to realize the operation characteristics of AC low-voltage microgrids.

Key-Words: - Microgrids, Distributed Generators, Steady-State Analysis, Three-Phase Power Flow, Distribution Systems.

1 Introduction

The electrical power system is usually divided into three segments which are generation, transmission, and distribution. Under the traditional structure, the large fossil-fuelled steam power stations, together with nuclear power plants and hydro stations, provide the majority of electrical energy. Thus the CO_2 emission of the large thermal power plants cause global warming to become increasingly worse. Besides, the efficiency is low due to the transmission losses. Consequently, one of the major tasks of mitigating the global warming phenomenon is reducing the power generation of such thermal units and to simultaneously increase the penetrations of DGs.

Up to now, commercially operating DGs, including solar energy, wind power, hydraulic power, geothermal power, etc., have the advantages of low environmental effect and high efficiency. DGs have smaller capacity compared with larger thermal power plants. These kinds of units are suitable for connected into medium-voltage or low-voltage distribution systems, and they can supply power near the load centre to meet the customer's demands. Distribution networks integrated with multiple DGs and loads are called microgrids, as shown in Fig. 1. Microgrids are able to operate under autonomous and grid-connected modes. This predominance can also compensate for the disadvantages of traditional centralized power systems with high emission and low efficiency. Furthermore, microgrids can also enhance power system reliability and power quality under optimal control and operation conditions. Since microgrids will play the vital important role in power systems in the future, it is necessary to realize the operation and nature of microgrids. Therefore, recent studies was focus on the related issues, such as optimal reactive power planning of doubly fed induction generators[1], integrated renewable sources for supplying remote power systems[2], power flow control strategy of dispersed generation[3], PV distributed generation penetration limits in LV distribution networks[4], effects of renewable distributed generation on distribution systems[5], power flow simulation of autonomous microgrids[6], etc. In which Power-flow analysis is the most fundamental of all system steady-state analyses in the system planning and operation stages. Additionally, low-voltage microgrids are inherently imbalanced; therefore, a rigid three-phase power-flow analysis is essential in order to reflect the physical phenomenon of real system. The major point of this paper is to analyze steady-state nature

of a low-voltage AC microgrid by sequential three-phase power-flow analysis based on the daily load curves.

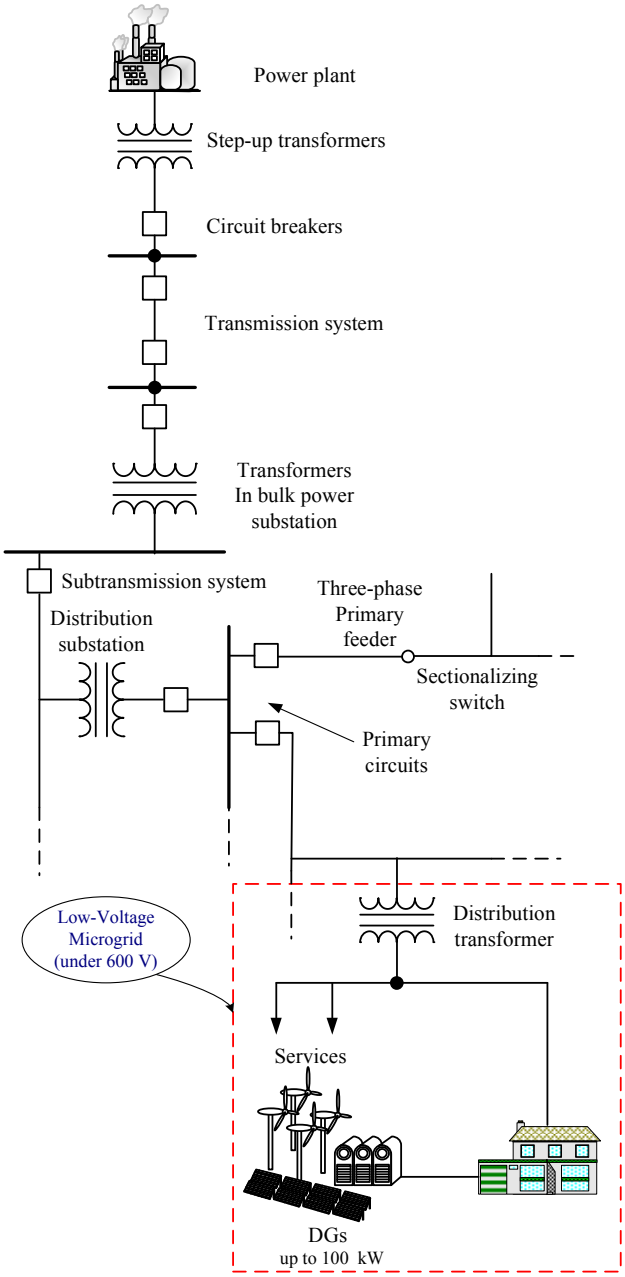

Fig.1 Schematic diagram of the low-voltage microgrid

2 Description of the Sample System

The low-voltage microgrids normally operate in a grid-connected mode through the MV/LV distribution transformer. Fig. 2. shows the sample system in this paper, this system was modified from the EU project "Microgrids" with Contract ENK5-CT-2002-00610 [7-8]. There are 14 buses in this system, and the longest distance from Bus 1 to Bus 10 is 345 m. Bus 1 is assigned as the swing bus. The remaining buses are load buses, namely, Bus 8 (residential load), Bus 9 (residential load), Bus 10 (industrial load), Bus 12 (commercial load), and Bus 13 (residential load). The system also includes representative sources from currently important technologies such as photovoltaics (PV), microturbines (MT), wind turbines (WT), and fuel cells (FC). For the simulation, the total installed capacity of the DGs is approximately 63 kW. The locations and capacities of the DGs interconnected to the network are as follows:

- A 10 kW photovoltaic generation system and a 10 kW wind turbine generator are connected to Bus 9 with three-phase inverter.
- A 10 kW fuel cell generation system is connected to Bus 10 with three-phase inverter.
- A 30 kW microturbine generator is connected to Bus 12 with three-phase inverter.
- In Phase A, a 3 kW photovoltaic generation system is connected to Bus 13 with single-phase inverter.

This sample system is used to simulate the transformer loadings, voltage profiles, line flow profiles, and system losses before and after the DGs are interconnected to the microgrid. Besides, the parameters of the distribution transformer, conductor, generation, and load are described in the following subsections.

2.1 Distribution Transformer

The related parameters for simulation of the MV/LV distribution transformer are listed in Table 1. This transformer is 400 kVA, 20 kV/0.4 kV, and its leakage impedance is 0.01+j0.04 *pu*.

2.2 Line Data

The impedance data for corresponding conductors are shown in Table 2. The ohmic value of the line impedance is recomputed in per unit value base on the same base values of apparent power, voltage, and impedance.

Table 1 MV/LV Distribution Transformer

Capacity (kVA)	Primary Side (kV)	Secondary Side (kV)	R(pu)	X(pu)
400	20	0.4	0.01	0.04

Table 2 Impedance Data for the Microgrid

Conductors	***Rph (Ω/km)***	***Xph (Ω/km)***
OL – Twisted cable 4x120 mm^2 A1	0.284	0.083
OL - Twisted cable 3x70 mm^2 A1+ 54.6 mm^2 AAAC	0.497	0.086
SC - 4x6 mm^2 Cu	3.690	0.094
SC - 4x16 mm^2 Cu	1.380	0.082
SC - 4x25 mm^2 Cu	0.871	0.081
SC - 3x50 mm^2 A1+35 mm^2 Cu	0.822	0.077
SC - 3x95 mm^2 A1+35 mm^2 Cu	0.410	0.071

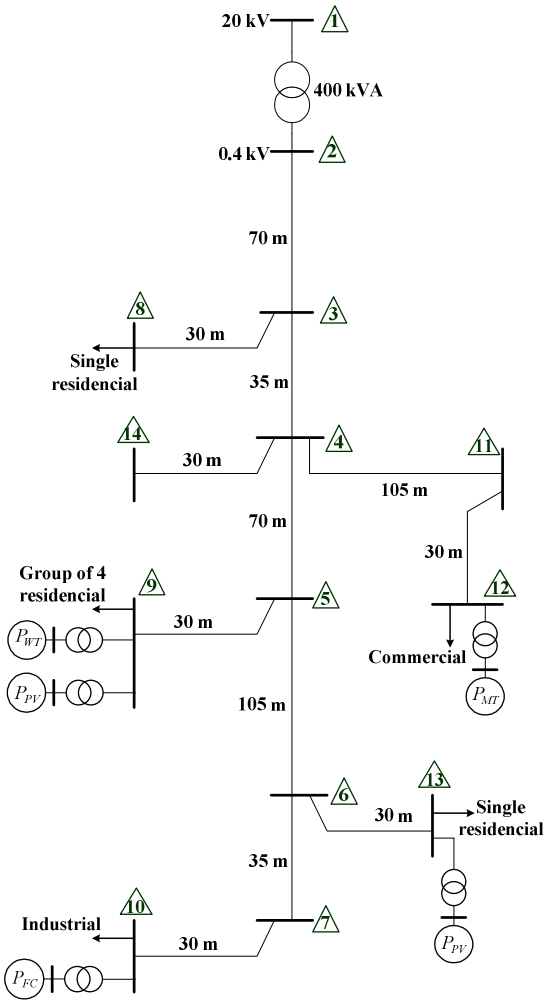

Fig.2 Single-line diagram of the low-voltage microgrid

2.3 Generation Data

Fig. 3 shows the real power output curves for four types of the DGs, where the power generations of the PV and WT are calculated by the proposed formulas in [9-11] with insulation, temperature, and wind speed-related parameters. Additionally, the power generated by the fuel-cell generation system and microturbine generator is calculated under the minimization of total fuel cost in the microgrid by direct search method. These curves are used as the power generation data for a full day's analysis.

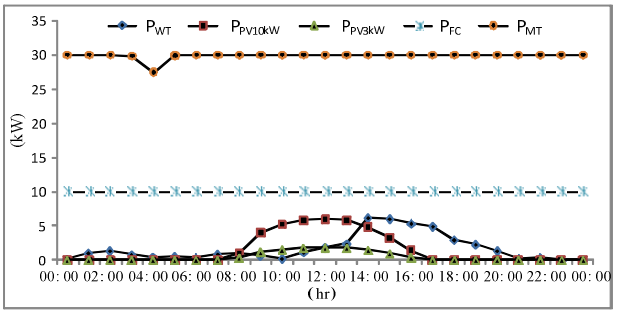

Fig. 3 Real power output curves for four types of DGs

2.4 Load Data

The typical daily load curves for three load types, namely, residential, industrial, and commercial are shown in Fig. 4 [8]. Besides, The peak loadings at each load bus are listed in Table 3. The above-mentioned load patterns and peak loadings are computed, and the results are utilized to draw the corresponding real and reactive daily load curves for each load bus in the microgrid, as shown in Fig. 5 and 6, respectively.

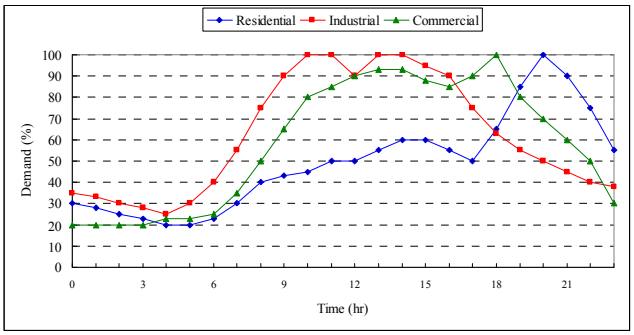

Fig. 4 Daily load curves for the three load types of the microgrid

Table 3 Peak Loadings for Three Load Types

Bus No.	*Phase A*		*Phase B*		*Phase C*	
	(kW)	(kvar)	(kW)	(kvar)	(kW)	(kvar)
Bus#8	4.25	2.63	4.25	2.63	4.25	2.63
Bus#9	15.58	9.66	15.58	9.66	15.58	9.66
Bus#10	13.32	8.25	13.32	8.25	13.32	8.25
Bus#12	20.40	12.64	20.40	12.64	20.40	12.64
Bus#13	4.25	2.63	4.25	2.63	4.25	2.63

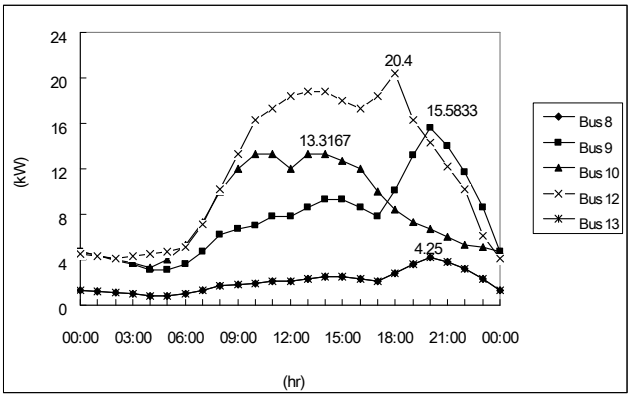

Fig. 5 Real power daily load curves for load bus (per phase)

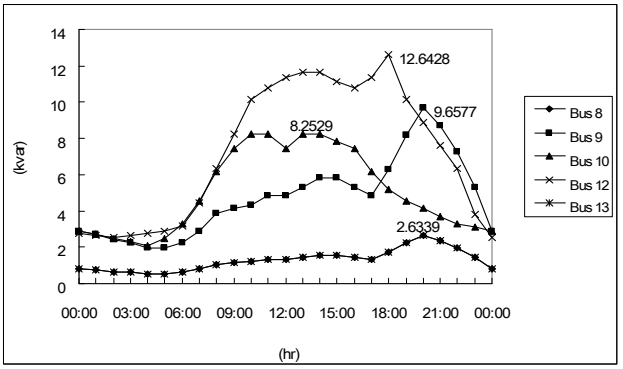

Fig. 6 Reactive power daily load curves for load bus (per phase)

3 Solution Approach

As mentioned above, the microgrids are the small power systems comprising various DGs and loads. These systems are inherently unbalanced due to the uncompleted three-phase line arrangements, loads, and different types of DGs. Related analytical techniques have been developed for distribution power flow solution[12-15], they have advantages and disadvantages in terms of accuracy, iteration number, execution time, memory storage, and so forth. Thus, a fast and effective solution is essential for a steady-state power flow, especially for the daily load analysis. Consequently, based on the implicit Z_{BUS} Gauss method [12], a sequential three-phase power-flow program was developed in this paper and is applied for performing sequential three-phase power flow. This approach is based on the principle of superposition, which is applied to the bus voltages along the feeders. The voltage on each bus is contributed from two different types of sources:

(1) the specified incoming bus voltage of the distribution substation;
(2) and current injections that are generated by the DGs, loads, capacitors, and reactors.

The solution procedure for the proposed approach can be described as follows. First of all, initialize bus voltage estimates and build the Z_{BUS}; secondary, compute the bus current injections by (1) for DGs, loads, and shunt elements. And then calculate the voltage deviations due to the current injections by (2). Finally, apply voltage superposition principle by (3) and update each bus voltage. In which V_{NL} denotes the no load voltage.

$$I_{i_{abc}}^{(k)} = \left(\frac{S_{i_{abc}}}{V_{i_{abc}}^{(k)}} \right)^{*} = \left(\frac{P_{i_{abc}} + jQ_{i_{abc}}}{V_{i_{abc}}^{(k)}} \right)^{*} \quad (1)$$

$$\left[\Delta V_{Bus}^{(k)} \right] = \left[Z_{Bus} \right] \cdot \left[I_{Bus}^{(k)} \right] \quad (2)$$

$$\left[V_{Bus}^{(k+1)} \right] = \left[V_{NL} \right] + \left[\Delta V_{Bus}^{(k)} \right] \quad (3)$$

The above solution procedure will be performed 24 times for a full day based on an hourly load and generation data. A flow chart of the proposed approach is illustrated in Fig. 7

4 Simulation Results and Discussions

The steady-state simulation results before and after the DGs interconnections are discussed in detailed in this section. The operation and nature of the low-voltage microgrids are explored and examined, after a thoughtful comparison and analysis of the transformer loadings, voltage profiles, line flow profiles, and system losses. First, the real power output curves for four types of the DGs are shown in Figure 3. Next, to proclaim the system imbalances under unbalanced loading conditions, the loads in the system are assumed unbalanced: 50% of the

three-phase loads on Phase A, 30% on Phase B, and 20% on Phase C. The simulation results are listed as follows.

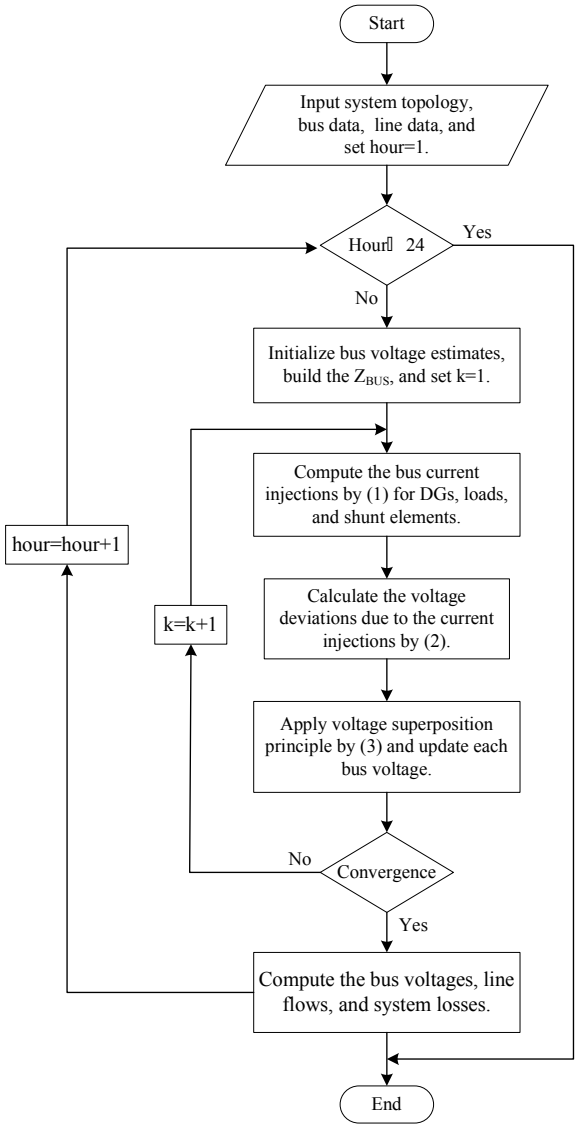

Fig. 7 A flow chart of the proposed sequential three-phase power-flow program

4.1 Distribution Transformer Loadings

After the DGs are connected to the network, the real power variations of the distribution transformer are obviously large as shown in Fig. 8; however, the reactive power variations are quite small, as shown in Fig. 9. This is primarily caused by the real power output of each DG supplying the nearby load demands, and the real power feed from the distribution transformer then being reduced. It should be noted that the real power is reversed to the primary distribution system through the distribution transformer in Phase C during the period of 0:00~06:00.

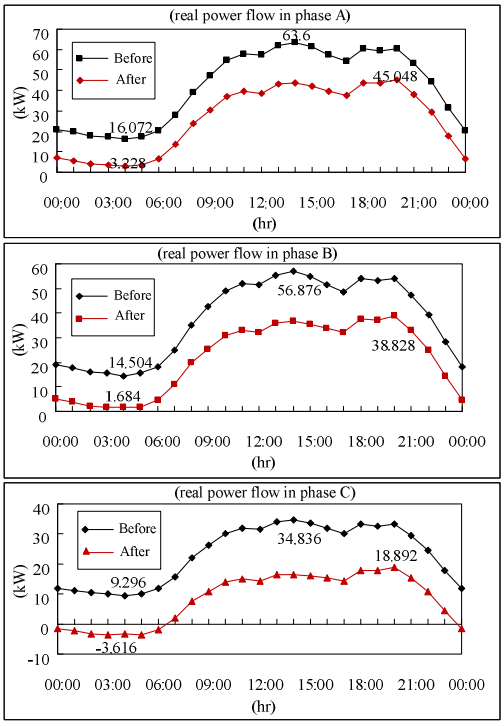

Fig. 8 Real power variations of distribution transformer before and after the DGs are connected to the network

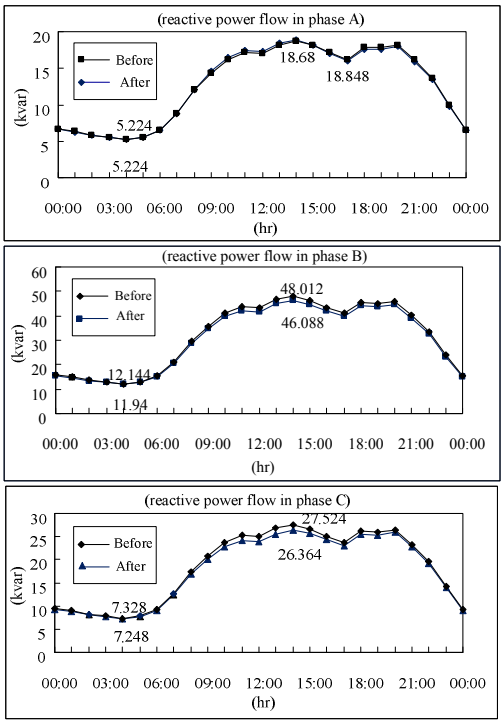

Fig. 9 Reactive power variations of distribution transformer before and after the DGs are connected to the network

4.2 Voltage Profiles

The simulation results of voltage profiles before and after the DGs are connected to the network are shown in Figures 10~15. The voltage variations at the secondary side of the distribution transformer (Bus 2) and load buses (Buses 8, 9, 10, 12, and 13) are visible. The average daily voltages at each bus are increased. Since the power feed from the DGs is large, the variations of the line currents are therefore significant. Accordingly, the more the power from the DGs, the more the line current and voltage variations rise. Additionally, the voltage drops are improved after the DGs are connected to the network. However, almost all the loads of all the buses mentioned above are larger than 3% most of the time, except for Bus 2, especially in the relatively heavier loading phase, Phase A.

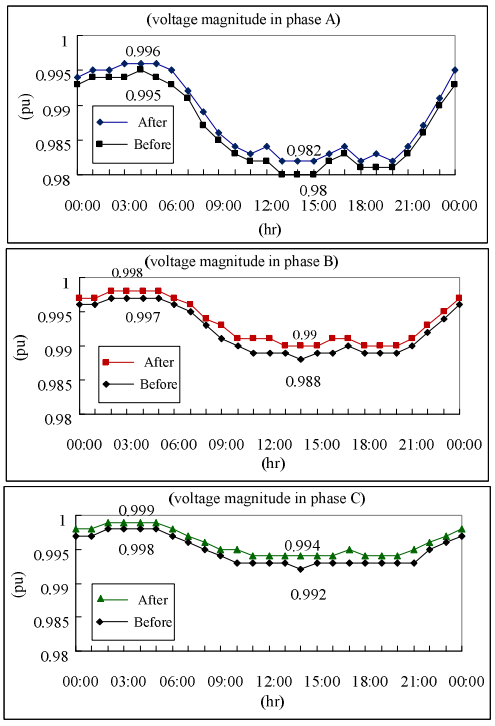

Fig.10 Voltage variations at Bus 2 before and after the DGs are connected to the network

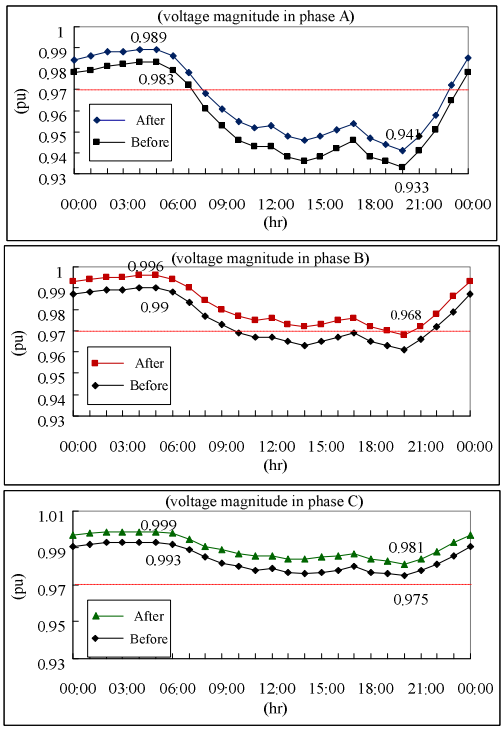

Fig. 11 Voltage variations at Bus 8 before and after the DGs are connected to the network

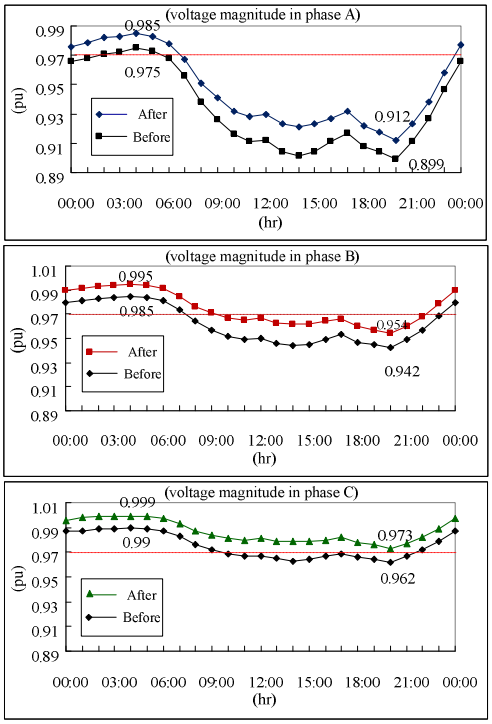

Fig. 12 Voltage variations at Bus 9 before and after the DGs are connected to the network

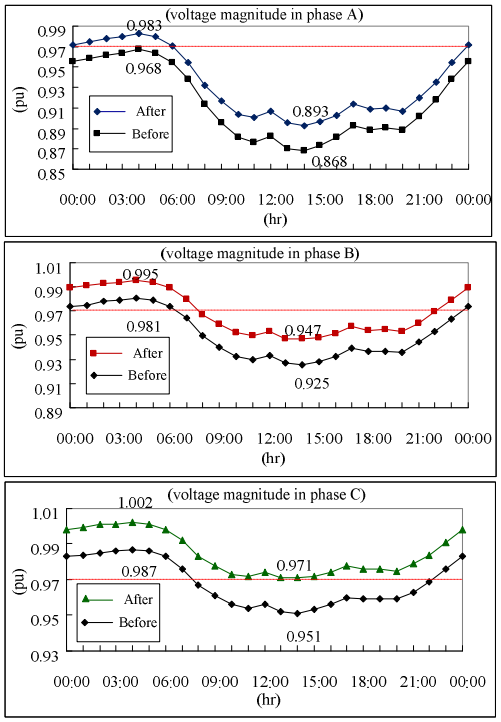

Fig. 13 Voltage variations at Bus 10 before and after the DGs are connected to the network

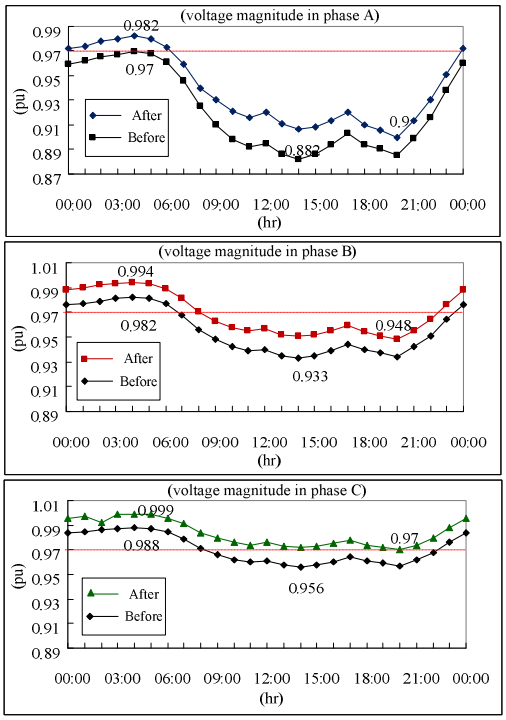

Fig. 15 Voltage variations at Bus 13 before and after the DGs are connected to the network

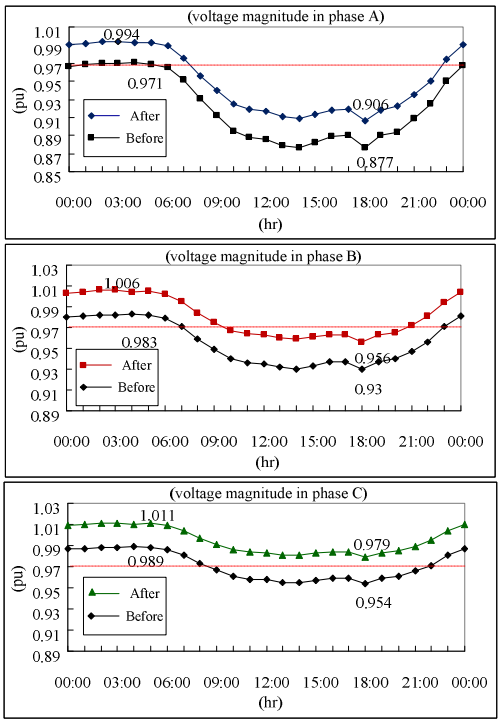

Fig. 14 Voltage variations at Bus 12 before and after the DGs are connected to the network

4.3 Line Flow Profiles

Figures 16~23 illustrate the variations of the real and reactive line flows in the line segment ahead of the DG connection point. After the DGs are interconnected, the variations of real power flow are significant. However, the variations of reactive power flow are quite small. The directions of currents in some line segments are reversed, and are directly proportional to the power from the DGs. Therefore, if the power from the DGs is increased, the conductors transfer mass power between the buses. This may lead to the conductors being overloaded, and the phenomenon should be avoided.

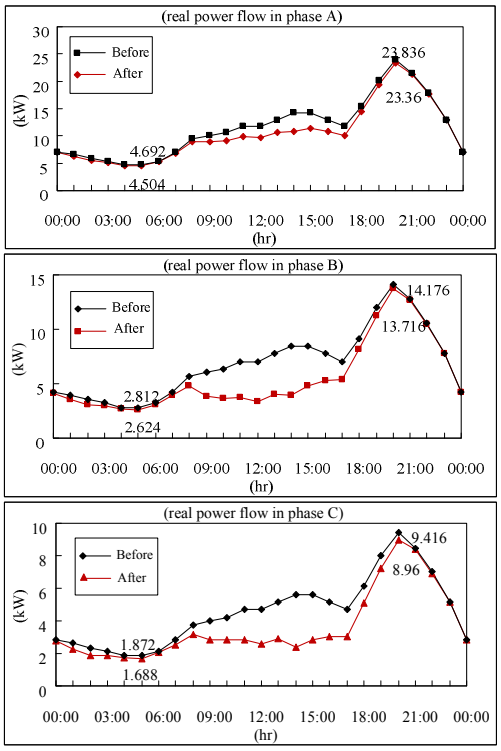

Fig. 16 Real-Power Line flow variations from Bus 5 to Bus 9 before and after the DGs are connected to the network

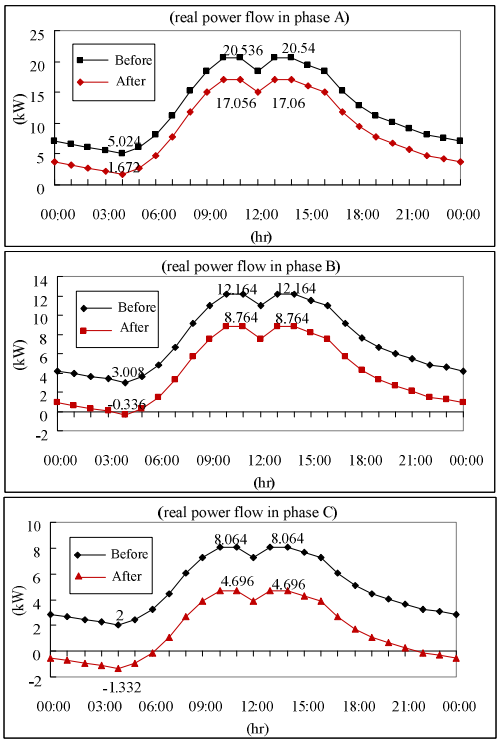

Fig. 18 Real-Power Line flow variations from Bus 7 to Bus 10 before and after the DGs are connected to the network

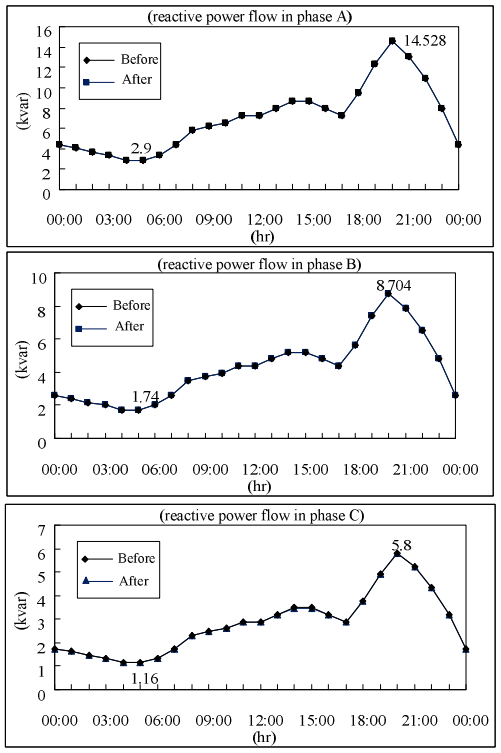

Fig. 17 Reactive-Power Line flow variations from Bus 5 to Bus 9 before and after the DGs are connected to the network

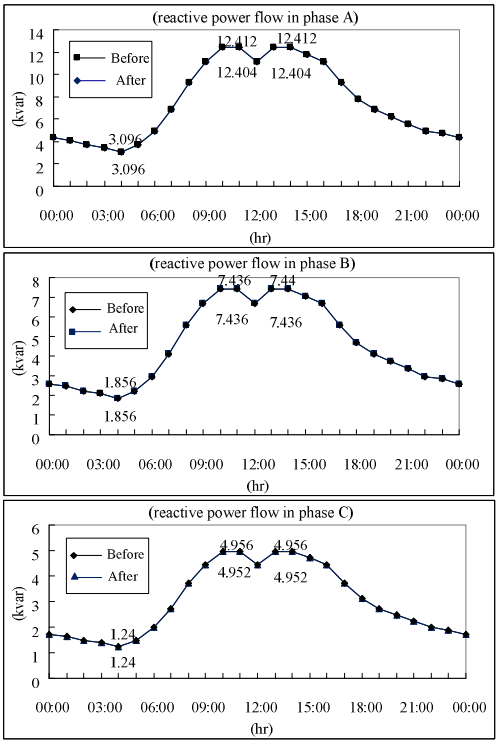

Fig. 19 Reactive-Power Line flow variations from Bus 7 to Bus 10 before and after the DGs are connected to the network

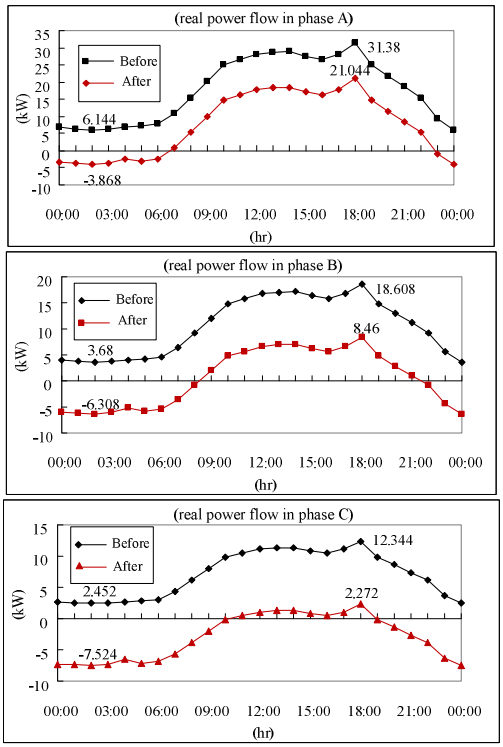

Fig. 20 Real-Power Line flow variations from Bus 11 to Bus 12 before and after the DGs are connected to the network

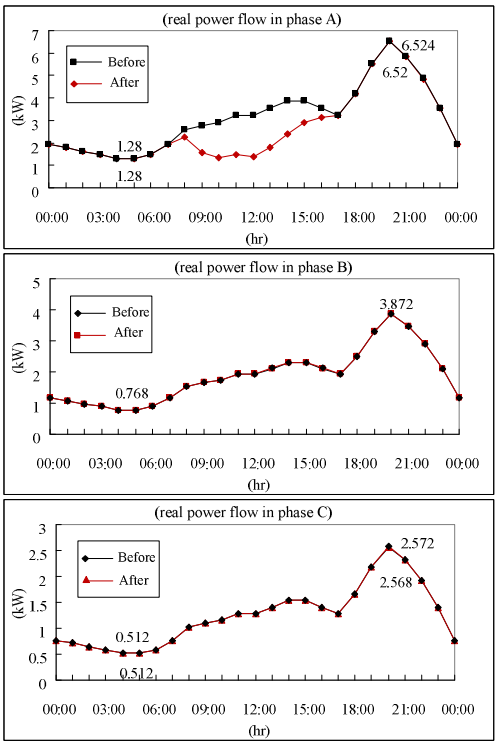

Fig. 22 Real-Power Line flow variations from Bus 6 to Bus 13 before and after the DGs are connected to the network

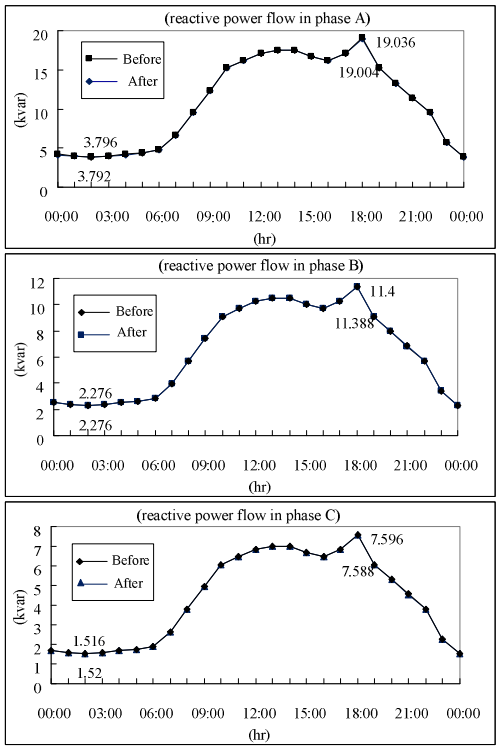

Fig. 21 Reactive-Power Line flow variations from Bus 11 to Bus 12 before and after the DGs are connected to the network

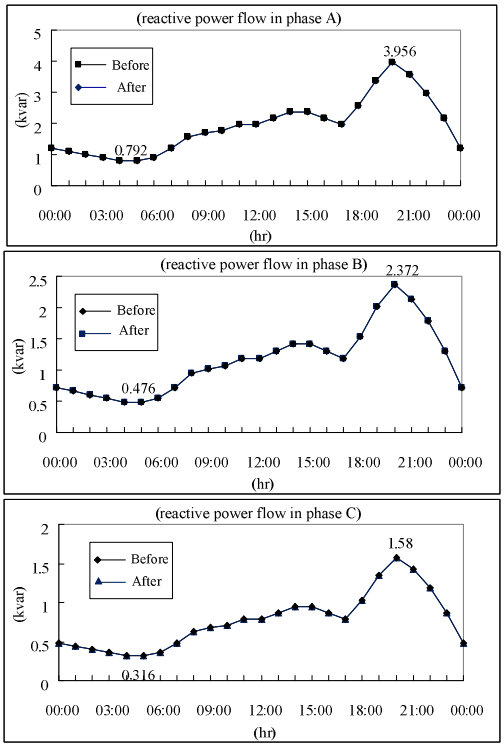

Fig. 23 Reactive-Power Line flow variations from Bus 6 to Bus 13 before and after the DGs are connected to the network

4.4 System Losses

Fig. 24 depicts the variations of the system losses before and after the DGs are connected to the network. The system losses are reduced after the DGs are connected to the network due to the DGs provide the power to meet customer's demands and reduced the power supply from the distribution transformer.

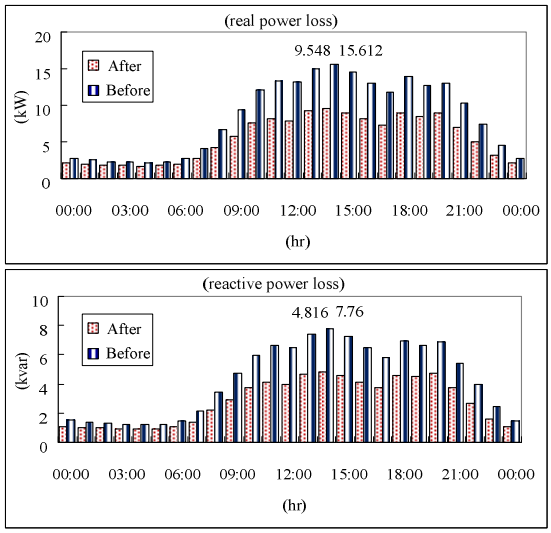

Fig. 24 System losses variations before and after the DGs are connected to the network

5 Conclusion

In this paper, based on the implicit Z_{BUS} Gauss method, the sequential three-phase power flow program is developed and tested to ensure its accuracy by commercial simulation package, CYME, and then performed the three-phase power flow analysis for a grid-connected low-voltage microgrid. The steady-state operation characteristics for a low-voltage AC microgrid with multiple DGs are then analyzed and discussed. To sum up the simulation results, after the DGs are connected to the microgrids, the average daily voltages at each bus are increased, and the tendency towards line flows and system losses is reduced. It is obvious that the DGs penetration increases the system operation efficiency and improves the voltage quality in this specific sample system.

6 Acknowledgement

The authors would like to thank the National Science Council of the Republic of China, Taiwan, for financially supporting this research under Contract No. NSC 97-2221-E-270-014-MY3 and Contract No. NSC 97-2221-E-149-010-MY3.

References:

[1] P. Sangsarawut, A. Oonsivilai and T. Kulworawanichpong, "Application of Genetic Algorithms for Optimal Reactive Power Planning of Doubly Fed Induction Generators," *WSEAS Transactions on Circuits and Systems*, Vol.9, Issue 3, 2010, pp.184-195.

[2] S. Leva, D. Zaninelli, and R. Contino, "Integrated renewable sources for supplying remote power systems," *WSEAS Transactions on Power Systems*, Vol.2, Issue 2, 2007, pp.41-48.

[3] A. Hanif and M. A. Choudhry, "Power flow control strategy at the load bus in the presence of dispersed generation," *WSEAS Transactions on Power Systems*, Vol.1, Issue.8, 2006, pp.1475-1483.

[4] S. Conti, A. Greco, N. Messina and S. Raiti, "Analytical vs. numerical analysis to assess PV distributed generation penetration limits in LV distribution networks," *WSEAS Transactions on Power Systems*, Vol.1, Issue.2, 2006, pp.350-357.

[5] Wen-Chih Yang, Tsai-Hsiang Chen, Jun-Den Wu "Effects of Renewable Distributed Generation on the Operational Characteristics of Meshed Power Distribution Systems," *WSEAS Transactions on Power Systems*, Vol. 4, Iss. 4, pp. 136-145, Apr. 2009.

[6] M. Wolter, "Power flow simulation of autonomous microGrids fed by renewable sources," *WSEAS Transactions on Power Systems*, Vol.1, Iss.11, 2006, pp.1911-1917.

[7] S. Papathanassiou, N. Hatziargyriou, K. Strunz, "A Benchmark Low Voltage Micro-grid Network" *Proc. CIGRE Symposium "Power Systems with Dispersed Generation"*, Athens, April 2005.

[8] EU Contract ENK5-CT-2002-00610, Technical Annex, "MICROGRIDS – Large Scale Integration of Micro-Generation to Low

Voltage Grids," May 2002, also http://microgrids.power.ece.ntua.gr

[9] M. M. Gilbert, "Renewable and Efficient Electric Power Systems," John Wiley & Sons, New Jersey, 2004

[10] M. J. Khan, M. T. Iqbal, "Dynamic modeling and simulation of a small wind–fuel cell hybrid energy system," Renewable Energy, Volume 30, Issue 3, Pages 421-439, March 2005.

[11] Website: http://www.cwb.gov.tw/V6/index.htm

[12] T. H. Chen *et al.*, "Distribution system power flow analysis - A rigid approach," *IEEE Trans. Power Del.*, vol. 6, no. 3, pp. 1146–1152, Jul. 1991.

[13] W. M. Lin, J. H. Teng, Three phase distribution network fast-decoupled power flow solutions, *International Journal of Electric Power & Energy Systems*, vol. 22, no.5, 2000, pp.375-380.

[14] U. Thongkrajay, N. Poolsawat, T. Ratniyomchai, T. Kulworawanichpong Unbalanced threephase distribution power flow using alternative Newton-Raphson method, *WSEAS Transactions on Circuits and Systems,* Vol.5, Issue 3, 2006, pp. 403-410.

[15] A. Augugliaro, L. Dusonchet, S. Favuzza, M. Ippolito, E. R. Sanseverino, "Direct Solution of Compensated Radial Distribution Networks with Constant Impedance/Current Loads," *WSEAS Transactions on Circuits and Systems,* Vol.8, Issue 1, 2009, pp. 1-10.